

Novel multi-layered systems with improved radar absorption

Jaume Calvo-de la Rosa^(1,2), Javier Tejada⁽¹⁾

jaumecalvo@ub.edu, javier.tejada@fmc.ub.edu

⁽¹⁾ Departament de Física de la Matèria Condensada, Universitat de Barcelona, Martí i Franquès 1, 08028 Barcelona, Spain

⁽²⁾ Institut de Nanociència i Nanotecnologia (IN2UB), Universitat de Barcelona, 08028 Barcelona, Spain

Abstract- The present work reports our recent advances on the development of new type of complex materials for improved broadband microwave absorption. Composite systems, containing powder functional magnetic components, have been build-up and optimized for stealth applications. Specific far field measuring systems have been designed, as well, to have a clear picture about the real performance of our materials. Experimental data and theoretical models are compared and discussed to have a full understanding of the absorption process. The results obtained so far show promising opportunities to enhance broadband radar absorption by means of multi-layered functional systems.

I. INTRODUCTION

Stealth technology is continuously gaining momentum due to its strong impact in fields such as communications, aviation, or military, to put some examples. The necessity to achieve electromagnetic isolation or to hide devices from radar detection systems drives the whole scientific community towards an ambitious technical challenge. New tools, systems and materials are required to face these goals.

There is a continuous search for materials capable to attenuate large amounts of radiation. In this regard, barium hexaferrite is one of the family of materials more studied so far. Due to the characteristics of the abovementioned sectors, lightness is crucial and, thus, high absorption by thin materials is desired. Nonetheless, it is still common to find in literature reports where thick samples (\sim mm) are used or they are not in their final application form, or even there is a lack of detail on how the absorption measurement is done. This makes imperative to progress on the design of new materials that satisfy the current necessities.

In this paper, we present our recent advances in the development of materials for stealth technology from two perspectives: (i) new experimental setups with improved capacities for characterizing radar absorbing systems, and (ii) novel materials with high broadband microwave absorption.

II. MATERIALS

The starting materials used for this study consist of magnetic powders of different nature. On one side, barium hexaferrite ($\text{BaFe}_{12}\text{O}_{19}$) powder was synthesized through a conventional coprecipitation route. We also modified this structure by the addition of further divalent cations, leading to the formation of magnetic nanocomposites with random magnetic properties [1]. Barium, iron and the added divalent cation (if it is incorporated into the structure) nitrates were

used as reactants (Scharlab, as received). On the other hand, metallic materials were provided by AMES S.L. and consist of micrometer-sized iron-based soft metallic powders [2].

These powder materials were mixed with paint or polymeric agents and deposited on top of $25\text{ cm} \times 25\text{ cm}$ polyester sheets of $50\text{ }\mu\text{m}$ thickness. Weight filling factor (ff_w), layer thickness and number of layers were controlled through mixing and deposition processes.

III. MICROWAVE MEASUREMENTS

One of our main goals was to develop an experimental setup to perform a precise dynamic electromagnetic characterization of materials and samples. Current literature that deals with the development of materials for stealth technology suffers from an important lack of adequate electromagnetic characterization systems. Despite a microwave absorbing material for radar applications is intended to coat a surface in the form of a film, most of the present studies work with bulk or powder samples [3], [4]. This is far from their final shape and requires meaningful and sensitive data post-processing. In addition, the vast majority of works perform the measurement in coaxial probes [5] or transmission lines [6], being far from the far-field conditions where the material will be applied. Finally, and most important, the most extended procedure in these references is to measure the relative permittivity (ϵ_r) and permeability (μ_r) of the sample and compute the reflection loss (R_L) from it, but not to measure R_L directly. In these cases, R_L is estimated by computing the impedance (Z) of a homogeneous medium:

$$Z = Z_0 \sqrt{\frac{\mu_r}{\epsilon_r}} \tanh \left[\left(j \frac{2\pi f d}{c} \right) \sqrt{\mu_r \epsilon_r} \right] \quad (1)$$

$$R_L (\text{dB}) = 20 \log \left| \frac{Z/Z_0 - 1}{Z/Z_0 + 1} \right| \quad (2)$$

From our perspective, all these assumptions and approximations may present a significant biasing between the computed values and the real performance of the materials. For this reason, our first mission has been to develop an experimental setup to perform a complete and precise electromagnetic characterization of materials and layers in the microwave frequency range. In addition to conventional coaxial probe measurements – which we have also used to characterize all the components individually, such as the polymers or the magnetic powders – we have built the system shown in Fig. 1. This system, connected to a VNA, allows for the direct measurement of layer-type

samples. Consequently, we can extract the complex permittivity and permeability of the samples in the same form in which they will be applied. Their intrinsic physical properties, geometrical characteristics, and fabrication artifacts are therefore considered in the measurement.

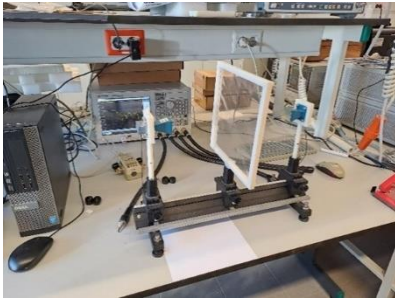


Fig. 1. Image of the experimental setup used in our measurements, consisting of two antennas connected to a VNA and a sample holder in between.

This system allows to perform a two-ports measurement of the complex S -parameters. The sample is subjected by the frame placed in the center of the setup, in perfect alignment with the two horn antennas. Together with the hardware part, we have also defined a specific signal processing algorithm to process the signal and account for losses. This type of measurement systems, as well as the Nicolson-Ross-Weir (NRW) method used later to compute complex ϵ_r and μ_r from S -parameters, are extremely sensitive to any signal or phase variation. This makes essential to account for any signal interference during the data processing, to ensure that the processed data only comes from the sample interference. Our algorithm accounts for multiple factors, such as environmental noise, internal reflections in the antennas, diffraction effects on the frame's borders or phase shifts along the wave path, for instance.

In addition to the previous, we are also convinced about the necessity of performing real radar experiments to contrast the R_L data that may be simulated from the sample's electromagnetic properties. Therefore, all our samples are also subject to an experimental measurement of the reflection loss in far-field conditions, simulating real radar conditions, inside an anechoic chamber. This setup is schematized in Fig. 2.

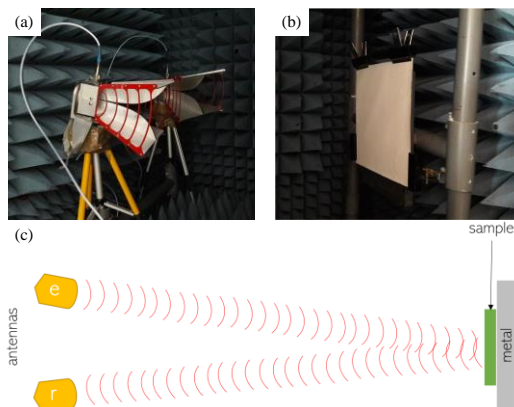


Fig. 2. Real pictures of the (a) antennas and (b) sample holder, and (c) scheme of the radar measurements done inside an anechoic chamber.

IV. RESULTS AND DISCUSSION

We always characterize all the samples by both methods, allowing the comparison between computed and experimental data. This also gives us the opportunity to analyze the results according to theory and models to have full understanding of the absorption mechanisms. In this manuscript, we present a selection of relevant results that we have obtained so far to exemplify the methodology and its capabilities.

Let us start with the electromagnetic characterization. All the prepared samples are first characterized with the experimental system depicted in Fig. 1. We start with a proper calibration and removal of noisy signals through signal processing, to be confident that the obtained complex S -parameter are only due to the sample's interference. Then, we process these data with the NRW method to obtain both the magnetic and the dielectric components of the samples at the microwave frequency range. These results are depicted in Fig. 3.

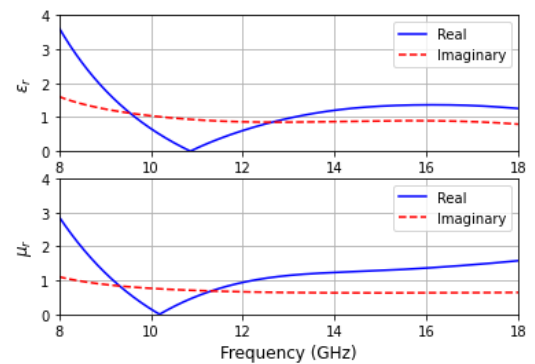


Fig. 3. Complex (a) permittivity and (b) permeability spectra obtained for a sample with Mn-Zn ferrite dispersed in PDMS ($ff_w = 75\%$) between 8 and 18 GHz.

Once the electromagnetic properties of all the samples are known, their absorption is measured in the anechoic chamber under real far-field radar conditions. There, we can measure the experimental absorption spectrum of the exact same sample characterized before. As an example, Fig. 4 represents, in blue, the microwave absorption spectrum obtained for the same sample analyzed in Fig. 3.

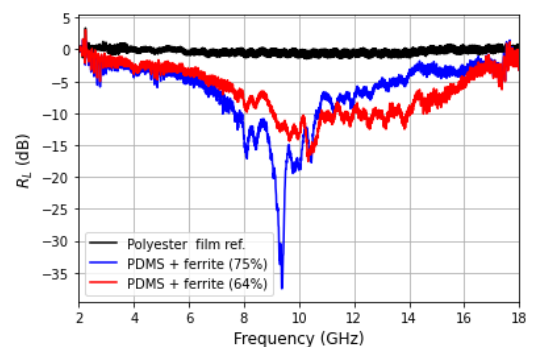


Fig. 4. Experimental R_L measured inside an anechoic chamber between 2 and 18 GHz. Blue line shows the results for the same sample shown in Fig. 3 ($ff_w = 75\%$) while the red one shows how properties change when $ff_w = 64\%$. Black line represents the absorption spectrum of the 50 μ m thick polyester sheet where the deposition is done, as reference.

In this figure we detect an interesting radar absorption performance for this sample has, reaching 35 dB at ~ 9.5 GHz while keeping an absorption of 15 dB along 2 GHz. However,

it is also possible to see how its absorbing properties may be modified with proper design, in this case by changing the ff_W . Other significant variables are the layer thickness or the electromagnetic properties of each component, for instance. The sample with a lower powder load does not provide such intense absorptions but shows a much broadband behavior. In this case, the sample absorbs 10 dB along 6 GHz (from 8 to 14 GHz, approximately). These results highlight the importance of a proper optimization and the versatility that can be achieved with these samples.

These results stick to the case of a single layer system, which is the scenario mostly considered by previous literature. However, for the first time, we are designing, preparing, and measuring the radar absorption capacities of multi-layered systems. With this new approach, we open a door for developing a new class of materials for stealth applications. Multi-layered systems, in contrast to traditional single layer ones, allow the search for the adequate coupling of the intrinsic physical and geometrical characteristics of the different layers. As demonstrated above, the options to tune the properties in a single layer are numerous, but a multi-layer system expands these opportunities to larger horizons.

As an example of how significant the incorporation of an additional layer may be, let us analyze Fig. 5. This figure shows the microwave absorption spectrum of two independent samples – one of them being already well known for its absorbing capacities [7] – as well as the results of their superposition.

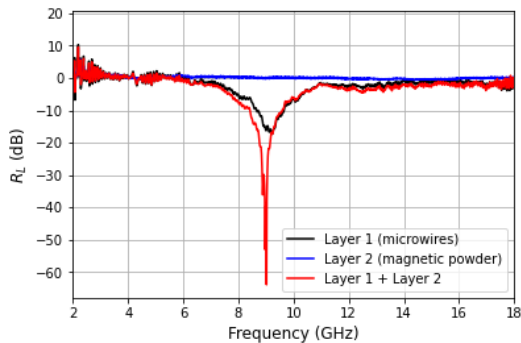


Fig. 5. Experimental R_L measured inside an anechoic chamber between 2 and 18 GHz. The response of two independent layers is plotted vs the result of their superposition.

These experimental data proved the strong potential that this new approach has. As it may be observed, there is one layer that does not absorb between 2 and 18 GHz and another one that absorbs 20 dB by its own. However, once superposed, more than 60 dB are achieved.

The superposition of two layers does not result in the superposition of their spectra. When this happens, we are in a complex scenario where there is an interaction between layers. The physical and geometrical coupling between the two layers is a powerful tool for improving the radar absorbing capabilities.

This scenario was studied by our team in collaboration with Prof. Chudnovsky [8], leading to a theoretical model capable to compute the reflection of a bi-layer system:

$$Z = -Z_0 \frac{\sqrt{\frac{\mu_1}{\epsilon_1}} \tanh\left(j\frac{2\pi\omega}{c}\sqrt{\epsilon_1\mu_1}d_1\right) + \sqrt{\frac{\mu_2}{\epsilon_2}} \tanh\left(j\frac{2\pi\omega}{c}\sqrt{\epsilon_2\mu_2}d_2\right)}{1 + \sqrt{\frac{\mu_1\epsilon_2}{\epsilon_1\mu_2}} \tanh\left(j\frac{2\pi\omega}{c}\sqrt{\epsilon_1\mu_1}d_1\right) \tanh\left(j\frac{2\pi\omega}{c}\sqrt{\epsilon_2\mu_2}d_2\right)} \quad (3)$$

This expression replaces (1) for bi-layered systems. With this model one can work on the optimization of each layer's thickness (d) and their corresponding electromagnetic properties (ϵ and μ), which are dependent on ff_W , to maximize the absorption. For fixed electromagnetic properties, for instance, it is possible to inspect the effect that the thickness of each of the two layers has on the reflection loss through the two-dimensional plot shown in Fig. 6.

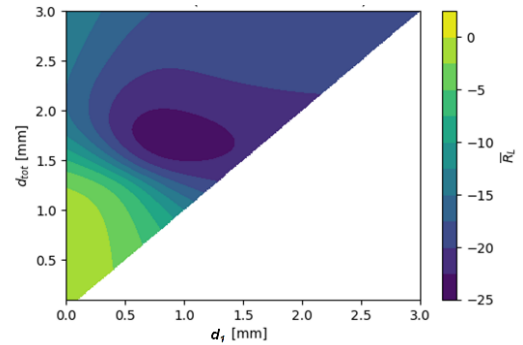


Fig. 6. R_L calculated with (3) for a given set of $\epsilon_1, \epsilon_2, \mu_1$ and μ_2 as a function of d_1 and d_2 . $d_{TOT} = d_1 + d_2$. \overline{R}_L represents the average R_L along 2-18 GHz.

This becomes to be an extremely powerful tool for the design process of new materials, which helps us on finding the most convenient conditions for a given system. At this point, it is important to point out that different criteria (i.e., the variable plotted on the color scale) can and must be depending on the specific application and necessity. In the case where a strong absorption is desired at a given frequency ω_i , the maximum R_L or $R_L(\omega_i)$ would be convenient choices; for broadband absorption, the averaged R_L (\overline{R}_L) or the frequency range with an R_L below a certain threshold should be used.

With all these tools in our hands, we have experimented with combinations of layers made by different materials, with different filling factors, different thicknesses, and different number of layers. The results are diverse, and we achieved systems capable to absorb in a wide variety of frequencies. In Fig. 7 we represent some cases where this versatility is seen. Each system represented here consists of the combination of different layers.

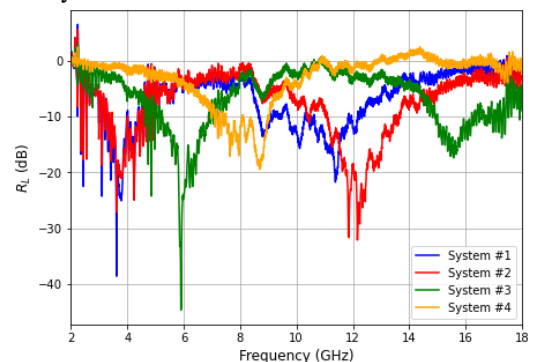


Fig. 7. Example of the experimental absorption spectra achieved by different systems.

We can observe cases with strong absorptions at ~ 4 , ~ 6 , ~ 8 , ~ 11 , ~ 12 and ~ 15 GHz, covering a large range of frequencies. In addition, the prepared systems have diverse behaviors, from those with very intense absorptions at specific frequencies to others with broadband losses. In the example in Fig. 7 we may even observe cases with a double peak present in the measured frequency range, increasing even more the possibilities for broadband absorbers.

V. CONCLUSIONS

The results presented in this paper are relevant from two perspectives. First, we have developed a new experimental procedure where both, a full electromagnetic characterization and a far-field radar measurement under real application conditions are done. This allows us to compare between experimental data and theory and represents a significant advance with regard current literature in terms of reliability of the experimental results. In addition to the experimental setup, the signal processing methodology that we have develop is crucial for a correct interpretation of the measured data. Strict calibration and corrections are required to ensure that only signals coming from the sample interaction are processed.

On the other hand, the results show that multi-layered systems open a new paradigm in the design of advanced materials for stealth applications. The coupling between layers, in addition to their intrinsic physical and geometrical properties, brings much more possibilities to our community. In this context, recent bi-layer impedance models become a crucial tool for the design of new systems and to extract fundamental understanding on the absorption mechanism.

Overall, the advances reported here represent a step forward from a fundamental science point of view, but from a practical and engineering perspective as well. New kind of materials and measuring methodologies with improved capabilities are incorporated into the field.

ACKNOWLEDGEMENTS

The authors acknowledge the financial support given by the U.S. Air Force Office of Scientific Research (AFOSR) through grant No. FA8655-22-1-7049. The authors also acknowledge Prof. Pilar Marin and Prof. Jose Maria López-Villegas for their collaboration.

REFERENCES

- [1] J. Calvo-De La Rosa, J. Manel Hernández, A. García-Santiago, J. Maria Lopez-Villegas, and J. Tejada, "Barium Hexaferrite-based nanocomposites as random field magnets for microwave absorption." doi: <https://doi.org/10.48550/arXiv.2402.14324>.
- [2] J. Calvo-de la Rosa, J. Tejada, and A. Lousa, "Structural and impedance spectroscopy characterization of Soft Magnetic Materials," *J Magn Magn Mater*, vol. 475, pp. 570–578, 2019, doi: 10.1016/j.jmmm.2018.11.085.
- [3] N. Shao *et al.*, "L and S band microwave absorption properties of Z-type hexaferrite Ba₃Co₂Fe₂₄O₄₁ synthesized at low temperature," *J Alloys Compd*, vol. 968, p. 171926, Dec. 2023, doi: 10.1016/j.jallcom.2023.171926.
- [4] K. P. Jeong, S. W. Yang, J. H. Choi, and J. G. Kim, "Microwave Absorption Characteristics of U-Type Ferrite Powders According to Substitution Elements and Its Compositions," *Metals and Materials International*, vol. 27, no. 8, pp. 2782–2790, Aug. 2021, doi: 10.1007/s12540-020-00613-z.
- [5] H. K. Choudhary, R. Kumar, S. P. Pawar, S. Bose, and B. Sahoo, "Effect of Microstructure and Magnetic Properties of Ba-Pb-Hexaferrite Particles on EMI Shielding Behavior of Ba-Pb-Hexaferrite-Polyaniline-Wax Nanocomposites," *J Electron Mater*, vol. 49, no. 3, pp. 1618–1629, Mar. 2020, doi: 10.1007/s11664-019-07478-y.
- [6] P. Kaur, S. Bahel, and S. B. Narang, "Broad-band microwave absorption of Sr_{0.85}La_{0.15}(MnZr)_xFe_{12-2x}O₁₉ hexagonal ferrite in 18–40 GHz frequency range," *J Magn Magn Mater*, vol. 460, pp. 489–494, 2018, doi: 10.1016/j.jmmm.2018.01.042.
- [7] P. Marin Palacios, A. Hernando Grande, D. Cortina Blanco, J. J. Gomez Rebollo, and J. Calvo Robledo, "Electromagnetic radiation absorber based on magnetic microwires," EP 1 675 217 A1, 2005
- [8] J. Calvo-de la Rosa *et al.*, "New Approach to Designing Functional Materials for Stealth Technology: Radar Experiment with Bilayer Absorbers and Optimization of the Reflection Loss," *Adv Funct Mater*, p. 2308819, Oct. 2023, doi: 10.1002/adfm.202308819.